Improvement of wire-mesh sensor accuracy via adapted circuit design and integrated energy loss measurement

OPEN ACCESS
IOP Publishing
Measurement Science and Technology
Meas. Sci. Technol. **33** (2022) 084002 (13pp)
https://doi.org/10.1088/1361-6501/ac6ab4

Improvement of wire-mesh sensor accuracy via adapted circuit design and integrated energy loss measurement

Felipe de Assis Dias[1,*], **Philipp Wiedemann**[1], **Eckhard Schleicher**[1], **Marco Jose da Silva**[2,3] and **Uwe Hampel**[1,4]

[1] Institute of Fluid Dynamics, Helmholtz-Zentrum Dresden-Rossendorf, Dresden, Germany
[2] Multiphase Flow Research Center, Universidade Tecnológica Federal do Paraná, Curitiba, Brazil
[3] Department of Electrical and Computer Engineering (CPGEI), Universidade Tecnológica Federal do Paraná, Curitiba, Brazil
[4] Chair of Imaging Techniques in Energy and Process Engineering, Technische Universität Dresden, Dresden, Germany

E-mail: f.dias@hzdr.de

Received 20 January 2022, revised 20 April 2022
Accepted for publication 26 April 2022
Published 5 May 2022

Abstract

We reviewed the electronic principles and design of the wire-mesh sensor with respect to inherent energy losses. From the analysis we derived a new circuit design with an optimized amplifier circuit and extended the sensor by an extra transmitter electrode embedded into the dielectric construction material. The latter allows an inherent determination of the energy losses that cannot be suppressed by circuit optimization only. Experimental analysis showed that we achieve an improvement in measurement accuracy with respect to the local and average phase fractions. Deviations in a single crossing point are reduced from more than 30% down to less than 5% and deviations in the average phase fraction are reduced from more than 15% down to less than 2%.

Keywords: wire-mesh sensor, multiphase flow, impedance measurement, energy loss correction

(Some figures may appear in colour only in the online journal)

1. Introduction

The wire-mesh sensor (WMS) is an instrument to measure the phase distribution of multiphase fluids in cross-sections of vessels and pipelines. It is an impedance-based sensor and was initially proposed for measurement of two-phase flows containing at least one conductive phase [1]. Over recent years, it has been improved to deal with non-conducting fluids [2], slurry flow [3] and also three-phase flows [4–6]. Although WMS is a slightly intrusive device, five major characteristics have contributed to its wide use in the scientific and industrial communities in the last twenty years: (a) high temporal resolution: frame rate up to 10 000 fps; (b) high spatial resolution: typically 2–5 mm; (c) safety: no radiation hazard; (d) versatility: it can be manufactured with different shapes and sizes from miniature versions [7] to sensors with inner diameter greater than 1 m. Additionally, it can be easily adapted to the process and some versions are suitable to operate at high temperatures and pressures of up to 400 °C and 10 MPa, respectively [8]); (e) easy post-processing: WMS provides local measurements that can be directly associated with at least one electrical

* Author to whom any correspondence should be addressed.

parameter of the fluid, e.g. electrical conductivity and relative permittivity. Therefore, no inverse problem algorithm is required.

Despite these advantages, WMSs may present some nonlinear behaviors resulting for example in the estimation of locally negative phase fraction [9, 10], which has no physical meaning. The most accepted procedure to deal with this issue is the use of a threshold method. Here, phase fractions greater than 1 and smaller than 0 are cut-off, leading to average phase fraction deviations within 10.5% compared to other measurement techniques [10]. However, the effectiveness of this approach is reduced if the flow is composed of dispersed phases. As detailed in [11], one of the causes of negative void fraction may be associated with temperature changes of the flow. Hence, a theoretical basis for temperature compensation and sub-models suitable for different types of fluids were provided to address this problem.

More recently, some works based on numerical simulation have pointed out that nonphysical estimations such as negative phase fraction can be also associated with the breaking of symmetry of the electric field [9] or the non-uniformity of the potential field generated by the sensor [12]. In this direction, it was found that the employment of different mixing models instead of the standard parallel (linear) model can somehow attenuate such nonlinear effects. In [9], the Maxwell model without cut-off procedure is recommended for gas-water flow containing dispersed phases, i.e. bubble flow. In [13], experiments suggested that Maxwell–Garnett and logarithmic mixture models are more suitable for intermittent oil-water flows. In [14], the logarithmic model is used in a reconstruction algorithm not only to improve the spatial resolution, but also to correct the phase fraction estimation of WMSs with a reduced number of electrode wires.

So far, much attention was paid to the investigation of different mixture models due to the assumption that one of the major sources of uncertainty is associated with the conversion from WMS raw data to derived flow parameters [10]. In fact, the use of different mixture models have improved the phase fraction estimation in some particular cases, as mentioned previously. However, they do not solve the source of the problem. According to Dias *et al* [15], the major source of uncertainty is actually associated with AC limitations of the amplification circuit, which was demonstrated experimentally and numerically through a WMS model that combines finite-element method (FEM) and SPICE simulation. In another work, Dias *et al* [16] suggested a procedure to tune the feedback gains of a WMS in order to improve the measurement accuracy of multiphase flows containing conductive fluids such as tap water. However, as will be discussed in this paper, this procedure does not hold for a broad range of conductivity if the current wire-mesh front-end circuits are used.

Hence, as a step in the further development of WMS technology, we propose in this paper a modified WMS with added reference impedances to compensate nonlinear effects of the amplifiers. Firstly, we provide a detailed review of the operating principle of WMS. The causes of energy losses and how they are associated to the amplification system are discussed in detail. Finally, the new method based on the modified WMS is presented and used to correct measurements effected by energy losses.

2. Theoretical background

2.1. Operating principle of WMS

Figure 1(a) shows a standard configuration of a WMS, where transmitter and receiver wires are crossed along the pipe wall forming a regular grid. The sensor measures the electrical properties of the fluids in a flow cross-section in the crossing points of the grid. As can be seen in figure 1(b), transmitter and receiver wires are perpendicular and separated by a small distance. The measurement is made by applying a voltage signal to a transmitter wire, which creates a potential difference between transmitter and receiver wires in a crossing point. This causes a current that is converted to voltage by a transimpedance amplifier. The output signal is a voltage proportional to the admittance of the fluid in the sensing volume of a crossing point. Hence, the measured quantity is an electrical current change as response to an input voltage change given by

$$\frac{\Delta U_{i,j,k}}{\Delta I_{i,k}} = Y_{i,j,k} \cdot Z_f, \tag{1}$$

where, Y is the admittance of the fluid and Z_f is the feedback gain. The indices i and j represent the line and column of a crossing-point, respectively, and k is the time (sample) index. As discussed in [17], the admittance of a fluid can be approximated as

$$Y = G + j\omega C = k_g \cdot (\sigma + j\omega\varepsilon_o\varepsilon) \tag{2}$$

where, G, C, σ and ε are the conductance, capacitance, conductivity and relative permittivity of the fluid, respectively, k_g is a geometry constant of the cell, ω is the angular frequency, ε_o is the vacuum permittivity and $j = \sqrt{-1}$ is the imaginary unit.

Based on this physical principle, different schemes have been proposed to determine at least one electrical property of the fluid, e.g. conductivity [1], permittivity [2] or both [4–6]. In all these modalities, the excitation mode is of the type $N \times 1$ as proposed in [1]. That is, the input signal is multiplexed by an analog switch, so only one transmitter wire is excited per time while the signal response of all receiver wires are measured simultaneously. This procedure is repeated sequentially for all transmitter wires, so that at the end of a measurement cycle, a matrix of local measurements of the flow cross-section is obtained. This excitation mode makes the sensor very fast, since only N time steps are necessary to acquire a frame. However, depending on the characteristics of the amplifiers and feedback gains, the amplification system might deviate from ideal, causing energy losses and crosstalk. Such problems are analyzed in detail in section 3 and a new method for energy loss correction is presented in section 4.

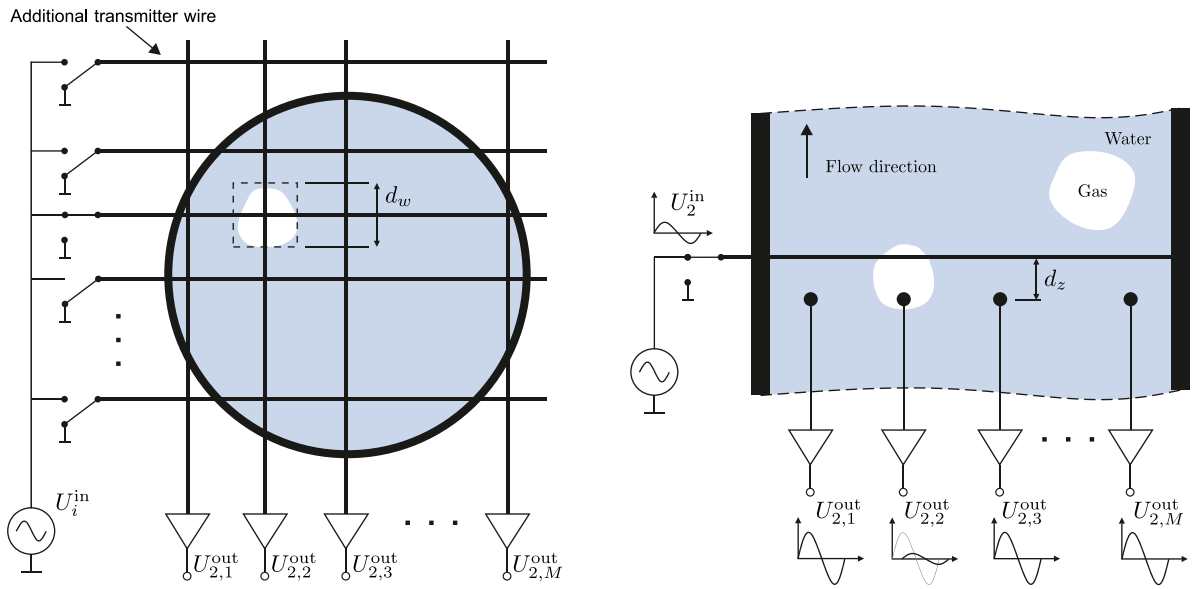

(a) Front view. (b) Lateral view.

Figure 1. Schematic and physical principle of a modified wire-mesh sensor (WMS) with an additional transmitter wire embedded into the PCB layout. A crossing-point outside the flow domain is used to measure the energy loss of the respective receiver wire. The procedure of loss correction is described in section 4.

2.2. Phase fraction calculation

The experiments presented in this paper were conducted with two WMSs. The first one is a 32×32 WMS with an inner diameter of 0.2 m (figure 2(a)). The second one is a 13×12 WMS with an inner diameter of 0.1 m (figure 2(b)). Although it is not visible in the photo, the latter contains an external transmitter wire embedded into the PCB layout outside the flow domain. Hence, only 12×12 electrode wires are stretched along the pipe cross-section. The external wire is used as reference for energy loss correction as will be detailed in section 4.

The WMS raw data were obtained through the data acquisition unit CAP200 (capacitance WMS [18]) provided by *TELETRONIC Rossendorf GmbH* [19]. The data are stored and sent to a standard PC for post-processing. To derive electrical and flow parameters from the raw data, i.e. electrical conductivity, permittivity or phase fraction, a calibration routine is required. In this work, only static calibration was used [1, 18], that is, two reference data sets are acquired prior to the experiments by filling the sensor with fluids with different electrical properties. Here, it was used water and air to generate the high and low calibration references, respectively.

Since the experiments were done with a capacitance WMS front-end [2], the raw data are digitized output voltages of the amplifiers in log scale given by

$$U_{i,j,k}^{(\log)} = a_{i,j} \cdot Y_{i,j,k} + b_{i,j}, \tag{3}$$

where, $a_{i,j}$ and $b_{i,j}$ are constants of the system related to the components used in the circuits. Here, the specific admittance of a crossing-point can be calculated as

$$Y_{i,j,k} = \frac{U_{i,j,k}^{(\log)} - b_{i,j}}{a_{i,j}}, \tag{4}$$

$$a_{i,j} = \frac{U_{i,j}^{(\mathrm{H},\log)} - U_{i,j}^{(\mathrm{L},\log)}}{\log(Y^{(\mathrm{H})}) - \log(Y^{(\mathrm{L})})}, \tag{5}$$

$$b_{i,j} = \frac{U_{i,j}^{(\mathrm{L},\log)} \cdot \log(Y^{(\mathrm{H})}) - U_{i,j}^{(\mathrm{H},\log)} \cdot \log(Y^{(\mathrm{H})})}{\log(Y^{(\mathrm{H})}) - \log(Y^{(\mathrm{L})})} \tag{6}$$

where, $U_{i,j}^{(\mathrm{H},\log)}$ and $U_{i,j}^{(\mathrm{L},\log)}$ are the high and low calibration references, and $Y^{(\mathrm{H})}$ and $Y^{(\mathrm{L})}$ are the theoretical admittances of the respective calibration fluids. The estimation of phase fraction based on electrical parameters such as conductivity, permittivity and admittance depends on how the phases of the flow are physically distributed inside a control volume [20]. Thus, different mixture models can be employed depending on the flow regime [4, 10, 13]. In this work, only the parallel model is used, so the void fraction is given by

$$\alpha_{i,j,k} = \frac{Y^{(\mathrm{L})} - Y_{i,j,k}}{Y^{(\mathrm{H})} - Y^{(\mathrm{L})}}. \tag{7}$$

The average void fraction is then calculated as

$$\overline{\alpha} = \frac{1}{K} \sum_i \sum_j \sum_k c_{i,j} \cdot \alpha_{i,j,k}, \tag{8}$$

where $c_{i,j}$ are weight coefficients to consider the shape of the pipe [21]. Due to energy loss, the results from equation (7) might provide nonphysical values greater than 1 and smaller than 0 [15, 16] and thus faulty values of $\overline{\alpha}$. The most used approach to deal with this problem is applying a threshold procedure such as

$$\alpha_{i,j,k}^{(\mathrm{th})} = \begin{cases} 1, & \text{if } \alpha_{i,j,k} > 1 \\ 0, & \text{if } \alpha_{i,j,k} < 0 \end{cases}. \tag{9}$$

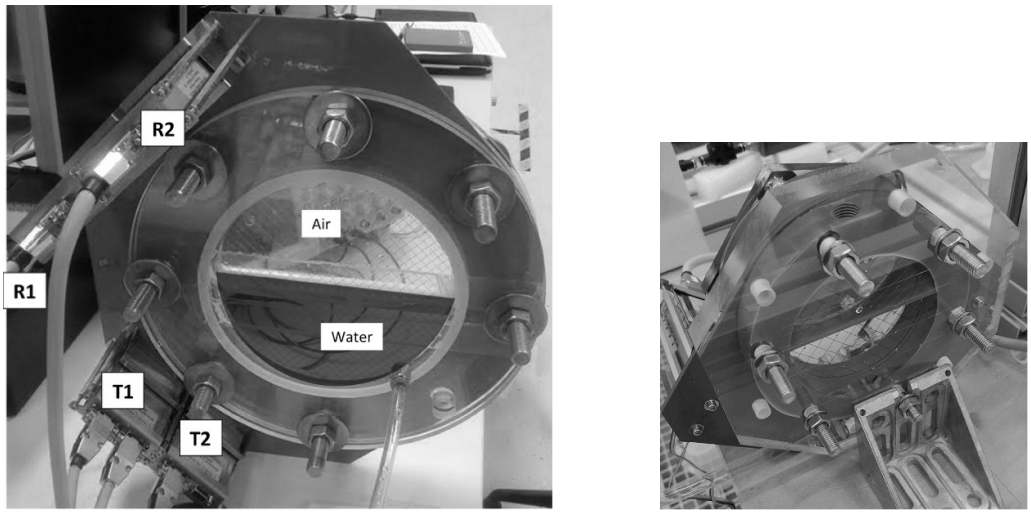

(a) (b)

Figure 2. WMSs used for the experiments in this study. (a) 32 × 32 WMS with inner diameter of 0.2 m (8 inch). (b) 12 × 12 WMS with inner diameter of 0.1 m (4 inch).

As one of the objectives of this work is to investigate the causes of negative fraction, equation (9) will be used only for comparison.

3. Analysis of energy loss and crosstalk

3.1. Basic considerations

In a conductive fluid the electrical current can go along different paths between the receiver and transmitter electrodes of a WMS as shown in figures 3(a) and (b). This arrangement can be represented as an electrical circuit (figure 3(c)), where $Z_{\text{eq}} = Z_{ct,1}||Z_{ct,2}||\ldots||Z_{ct,N}$ is the equivalent impedance of the neighboring crossing-points and C_{ct} is the stray capacitance from cables, PCB layout, etc. Assuming that the excitation and amplification stages of a WMS are ideal, the measurement of Y_x (or the reciprocal Z_x) is not affected by Z_{eq} and C_{ct}, since the negative input of the amplifier is at virtual ground and the deactivated transmitter wires are physically grounded. In this case, the transfer function of the measurement is given by

$$H_{i,j}^{(\text{ideal})} = \frac{U_{i,j}^{(\text{out})}}{U_j^{(\text{in})}} = -\frac{k_{g_{i,j}} \cdot Y_{i,j}}{R_f^{-1} + j\omega C_f}. \tag{10}$$

where, R_f and C_f are the resistor and capacitor in the feedback loop of the op amp, respectively, and $H_{i,j}^{\text{ideal}}$ is the ideal closed loop gain.

In real applications, however, the amplifiers are non-ideal. Depending on the frequency, bandwidth and conductivity of the fluid, the amplifiers may become unbalanced and the virtual ground does not hold. Hence, energy losses and crosstalk are not fully suppressed and $Y_{i,j}$ cannot be easily determined as in the ideal assumption. To consider such effects, the amplification stage of a WMS can be modeled as a non-ideal amplifier with a dominant-pole [22], which is given by

$$H_{i,j}^{(\text{nonideal})} = \frac{H_{i,j}^{(\text{ideal})}}{1 + \dfrac{1}{a(j\omega)\beta(j\omega)}}. \tag{11}$$

Here, the open-loop gain is approximated as

$$a(j\omega) = \frac{a_o}{1 + \dfrac{j\omega}{\omega_c}}, \tag{12}$$

where, a_o and ω_c are the DC gain and cut-off frequency, respectively. The *feedback factor* [16, 22, 23] is given by

$$\beta(j\omega) = \frac{Z_f^{-1}}{Z_f^{-1} + Y_{i,j} + Z_{\text{eq}}^{-1} + j\omega C_{\text{ct}}}, \tag{13}$$

and the amplification error can be estimated as

$$\epsilon_{i,j} = 100 \cdot \left(\frac{1}{1 + \dfrac{1}{a(j\omega)\beta(j\omega)}} - 1 \right) [\%], \tag{14}$$

which indicates the departure of a non-ideal op amp to ideal.

3.2. Effects of the bandwidth on the WMS

By inspecting equations (11)–(14) becomes clear that if a_o goes to infinity, the measurement of $Y_{i,j}$ becomes independent of β and the amplification error tends to zero. However, high-speed amplifiers have finite gain-bandwidths (GBW), which are typically lower than 10^6 MHz (unity-gain stable). To demonstrate the effects of the finite GBW on the output voltage of a WMS, the standard amplifiers in the receiver modules of a capacitance WMS were interchanged by op amps with GBW equal to 230 MHz and 145 MHz, respectively. Then,

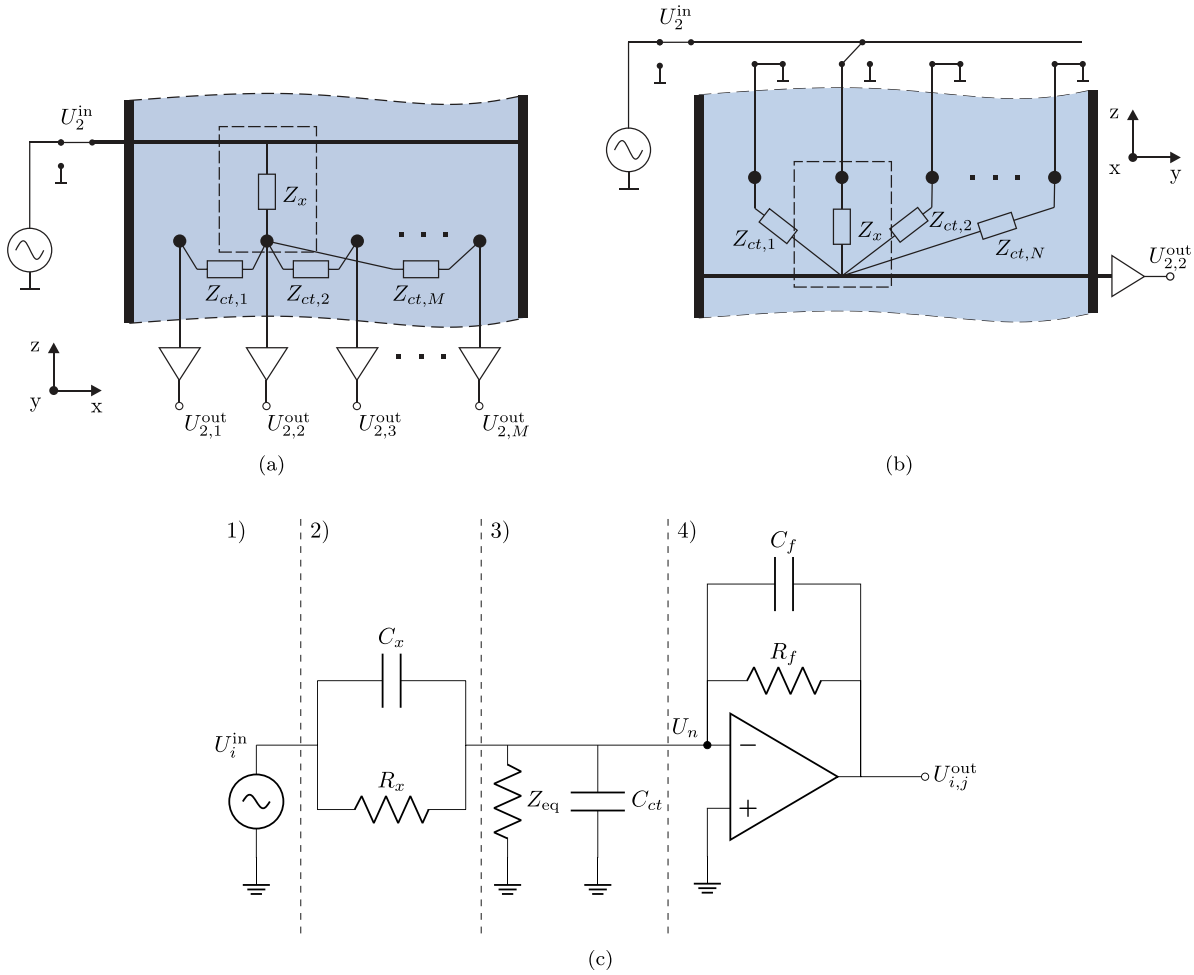

Figure 3. Effects of the neighboring crossing-points in WMS signals. (a) Impedance between receiver wires; (b) impedance between transmitter and receiver wires; (c) equivalent circuit model of a single channel of WMS composed by four parts: (1) excitation signal source; (2) impedance of the fluid in the control volume; (3) equivalent impedance of the neighboring crossing-points and stray capacitance; and (4) inverting amplifier.

two experiments were performed for each modified module with a 32×32 WMS filled with 50% deionized water. Figure 4 shows the experimental results.

As can be seen, figure 4(a) shows a strongly curved shape of the output signals when the sensor is filled with 100% of water (high calibration reference). The lower voltage signals are related to the crossing-points in the pipe center, since they are surrounded by a large volume of water. Hence, the equivalent impedance of the neighboring crossing-points Z_{eq} becomes much smaller than local measurements close to the pipe wall. In this example, it is clear that using amplifiers with a GBW equal to 145 MHz do not suppress the effects of Z_{eq} properly, so the energy losses in WMS becomes highly dependent on the liquid holdup. Consequently, a measurement where the sensor is filled with 50% water leads to voltage signals greater than the upper boundary (high reference). In this case, if equation (7) is used to convert WMS raw data to void fraction, values greater than 1 and smaller than 0 are obtained, as shown in figure 4(b).

In contrast, by using amplifiers with a higher gain bandwidth (230 MHz), the suppression of loss and crosstalk is improved, leading to an almost flat shape of the output signals for the high calibration data (figure 4(c)). As can be seen in figure 4(d), the number of local points containing values greater than 1 and smaller than 0 are reduced compared to figure 4(b), which highlights the importance of using amplifiers with a high bandwidth.

3.3. Effects of the feedback gain

The tuning of WMS gains is typically done by on-site calibration. For example, the sensor is filled with a conductive fluid and the gains are selected by changing the components R_f and C_f of the feedback loop in such a way that the largest signal is obtained. The goal of this approach is to ensure a high signal-to-noise ratio (SNR) in order to improve for example the discrimination of two non-conductive fluids such as gas and oil, or improving the measurement of flows with dispersed phases such as bubble flow. However, by increasing the closed-loop gain of an inverting amplifier, the frequency bandwidth is reduced, which is extremely undesirable as discussed in the previous section.

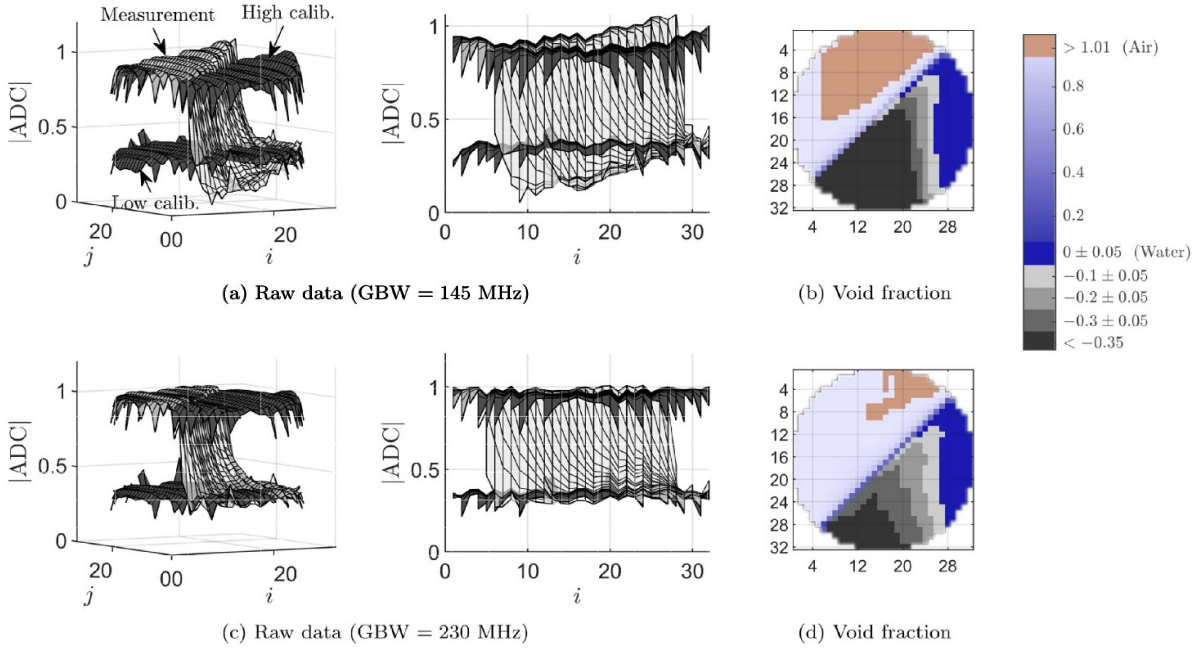

Figure 4. Conversion of raw data to phase fraction using the parallel model of the admittance of two-phase fluids. The data were acquired with a 32×32 WMS using two different amplifiers: (a) GBW = 230 MHz and (b) GBW = 145 MHz. The sensor is filled with 50% deionized water (1 μS cm^{-1}). The feedback loop of the amplifiers was set with the components $R_f = 30$ kΩ and $C_f = 2.2$ pF in both experiments. The indices i and j are the row and column of a frame, respectively.

Figure 5 shows several mappings of the gain error estimated by equation (14) as function of (R_f,C_f), conductivity of fluid and impedance of the mesh Z_{eq}. As Z_{eq} is unknown and depending on the phase distribution, it is reasonable to assume that the impedance of the mesh is given by $Z_{eq}{}^{-1} = Y_{eq} = \eta Y_x$, where Y_x is the admittance of an activated cell and η is a mesh factor. Here, a high η (e.g. 100) represents a sensor with very large inner diameter with several crossing-points submerged in a conductive fluid x.

As can be seen in the mappings, if a pair of R_f and C_f are selected in order to obtain output signals close to the upper limit of the amplifier (dashed line), the op amp deviates from ideal for most of the cases, that is, $\epsilon \gg 0.1\%$, mainly if the fluid's conductivity is too high or if the impedance of the mesh is too low (high η). Hence, the feedback gain has to be decreased for a proper operation, but at the cost of a lower SNR.

To evaluate the impact of high and low closed-loop gains on the phase fraction estimation, three combinations of (R_f, C_f) were chosen based on the mappings from figure 5. A high gain which is given by $Z_f = 13$ kΩ (30 kΩ, 2.2 pF) and two low gains obtained by increasing C_f, that is, $Z_f = 97$ Ω (30 kΩ, 330 pF) and decreasing R_f, as $Z_f = 89$ Ω (86 Ω, 2.2 pF). The experiments were performed using the 32×32 WMS shown in figure 2(a) containing 50% of water with three different conductivities: 1 μS cm^{-1}; 500 μS cm^{-1}; and 1000 μS cm^{-1}.

The void fraction distribution of each experiment is shown in figure 6. As can be seen, the combination of gain (30 kΩ; 2.2 pF) leads to high deviations for all experiments, as predicted by the mappings. In contrast, the occurrence of negative phase fraction is drastically reduced by increasing the capacitor C_f to 330 pF or reducing the resistor R_f to 86 Ω. Here, the average deviation of the cross-sectional void fraction of deionized (1 μS cm^{-1}) and tap water (500 μS cm^{-1}) were reduced from 30% to less than 5%. For salty water with conductivity of 1000 μS cm^{-1}, the average phase fraction deviation was reduced to less than 7%.

Figure 7 shows the local measurements along a chord of the sensor. It can be seen, that the use of a high feedback gain ($Z_f = 13$ kΩ) leads to local phase fraction deviations of up to -114%. In contrast, if Z_f is smaller than 97 Ω, the deviation is reduced to -5.2% for tap water. The deviation is considerably reduced also for deionized and salty water, however, the void fraction is overestimated in the former and underestimated in the latter, since the op amp starts to depart from ideal in such operating points.

These results confirm that the major source of uncertainty in WMS measurement is related to the first stage of amplification. However, only the optimization of the gains is not enough to suppress the losses caused by the amplifiers depending on the conductivity of the fluid and size of the sensor. For this reason, a new method to correct the energy losses is presented in the next section.

4. Novel method for energy loss correction using an adapted WMS

Due to the limitations of the optimization procedure described in the previous section, a new approach to correct energy

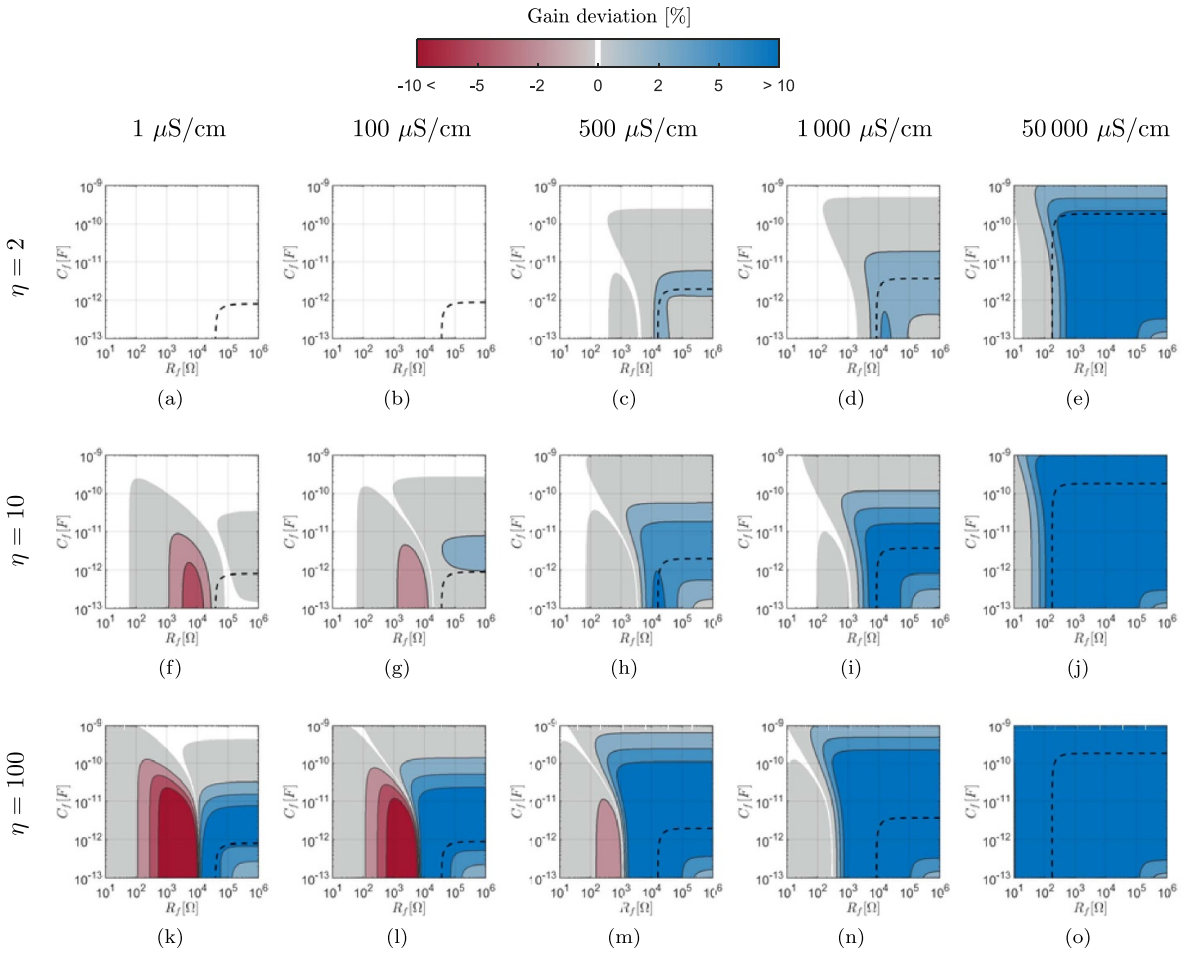

Figure 5. Gain error estimated by equation (14), which relates the fluid's conductivity, mesh factor η and the components (R_f, C_f). The mappings were calculated assuming a GBW = 230 MHz, $k_g = d_w^2 \cdot d_z^{-1}$ and $C_{ct} = 120$ pF [24]. The black dashed line is the upper limit of the output signal (4 dB) assuming an input signal of 1 V peak-to-peak (5 MHz).

losses in WMS signals is proposed (reference number of the patent application: [DE102021116540.7]). Here, a modified WMS arrangement is created to measure the losses caused by conductive fluids, which in turn are used to correct the readings of the sensor. Figure 1(a) shows a schematic of the sensor arrangement. It comprises an additional transmitter electrode embedded outside the flow domain into the PCB layout. Since the sensitivity volume of an external crossing-point has a constant dielectric (PCB layout), its signal response has to be constant. Hence, signal changes in the external crossing-points indicate the occurrence of losses, which can be compensated in further data processing. Based on this principle, a method to compensate such nonlinear effects is presented as follows.

4.1. Correction of energy loss

From equation (11) we can assume that a real measurement of WMS is given as

$$U_{i,j,k}^{(\mathrm{real})} = \frac{U_{i,j,k}^{(\mathrm{ideal})}}{\xi_{i,k}}, \tag{15}$$

where, $U_{i,j,k}^{(\mathrm{ideal})}$ is an ideal output signal and $\xi_{i,k}$ is a loss factor, which is associated with the electrical currents that can go along paths created by conductive fluids between transmitter and receiver wires. Here, two assumptions are made:

(a) For a measuring channel there is only energy loss if a conductive fluid creates a path between its receiver electrode to other wires $(\xi_{i,k} \neq 1)$;
(b) For non-conductive fluids such as air, the electrical current that goes through Z_{eq} is very small, so that the loss can be neglected $(\xi_{i,k} \approx 1)$;
(c) Assuming that the resistance of the wires are negligible, the coupling caused by a conductive fluid has the same impact in all crossing-points of the same receiver wire. Hence the loss factor can be assumed constant along a receiver wire, that is, $\xi_{1,i,k} = \xi_{2,i,k} = \ldots \xi_{M,i,k}$.

Based on assumptions (a) and (b), the loss factor of a receiver wire can be estimated as

$$\tilde{\xi}_{i,k} = \frac{U_i^{(\mathrm{air,ex})}}{U_{i,k}^{(x,\mathrm{ex})}}, \tag{16}$$

where, $U_i^{(\mathrm{air,ex})}$ and $U_{i,k}^{(x,\mathrm{ex})}$ are readings from the external crossing-points. The numerator of equation (16) is a reference

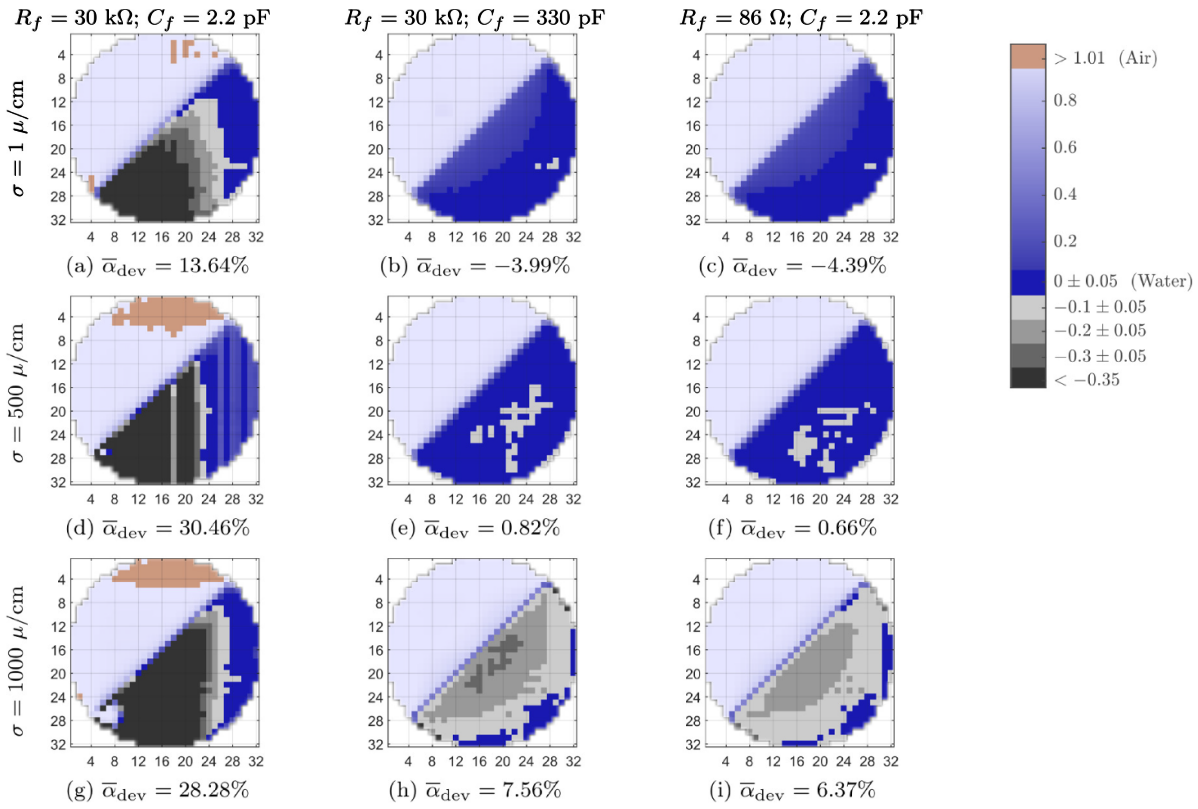

Figure 6. Phase fraction distribution estimated from 32 × 32 WMS data. The sensor is filled with 50% water as displayed in figure 2(a).

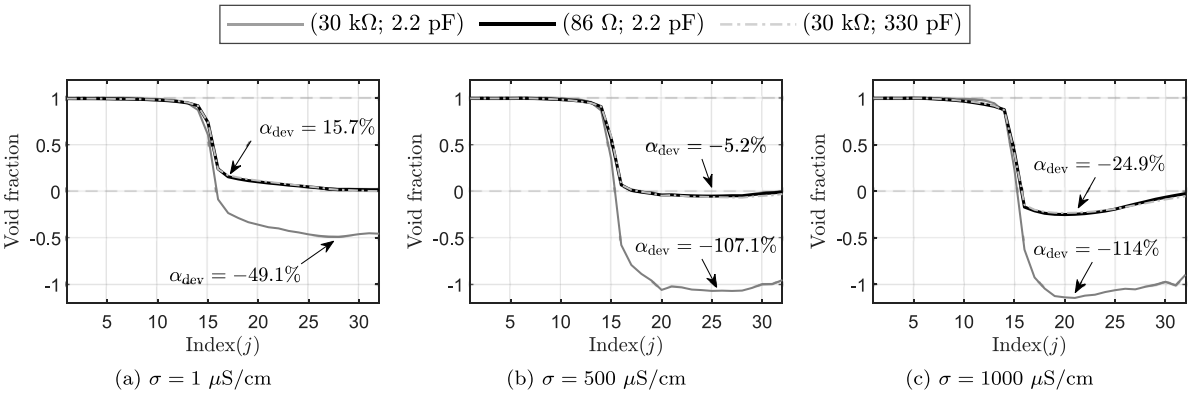

Figure 7. Local void fraction along a vertical chord of a 32 × 32 WMS ($i = 16$, $j = 1$–32) from figure 6.

signal obtained through a static calibration prior to the experiments by measuring a non-conductive fluid such as air. Here, there is no current path between the activated channel and the neighboring wires, so the loss is negligible (assumption (b)). Hence, equation (16) is a ratio that indicates how much measurement and reference signal deviate from each other due to losses. As the loss factor is constant along a given receiver wire (assumption (c)), the estimated loss factor can be used to correct signals from all crossing points related to the same receiver wire as

$$U_{i,j,k}^{(\text{corr})} = U_{i,j,k}^{(\text{real})} \cdot \tilde{\xi}_{i,k}. \tag{17}$$

By replacing (15) into (17), it is easy to see that the estimated loss factor $\tilde{\xi}_{i,k}$ compensates the real loss $\xi_{i,k}$. Thus, if assumption (c) holds, then the real measurement becomes closer to ideal.

As the output signals obtained with the data acquisition unit CAP200 are logarithmic scaled they have to be corrected as follows

$$a \cdot \log(\tilde{\xi}_{i,k}) = U_{i}^{(\text{air,log,ex})} - U_{i,k}^{(\text{log,ex})}, \tag{18}$$

and

$$U_{i,j,k}^{(\text{log,corr})} = U_{i,j,k}^{(\text{log,real})} + a \cdot \log(\tilde{\xi}_{i,k}), \tag{19}$$

where a is the same circuit constant calculated by equation (5).

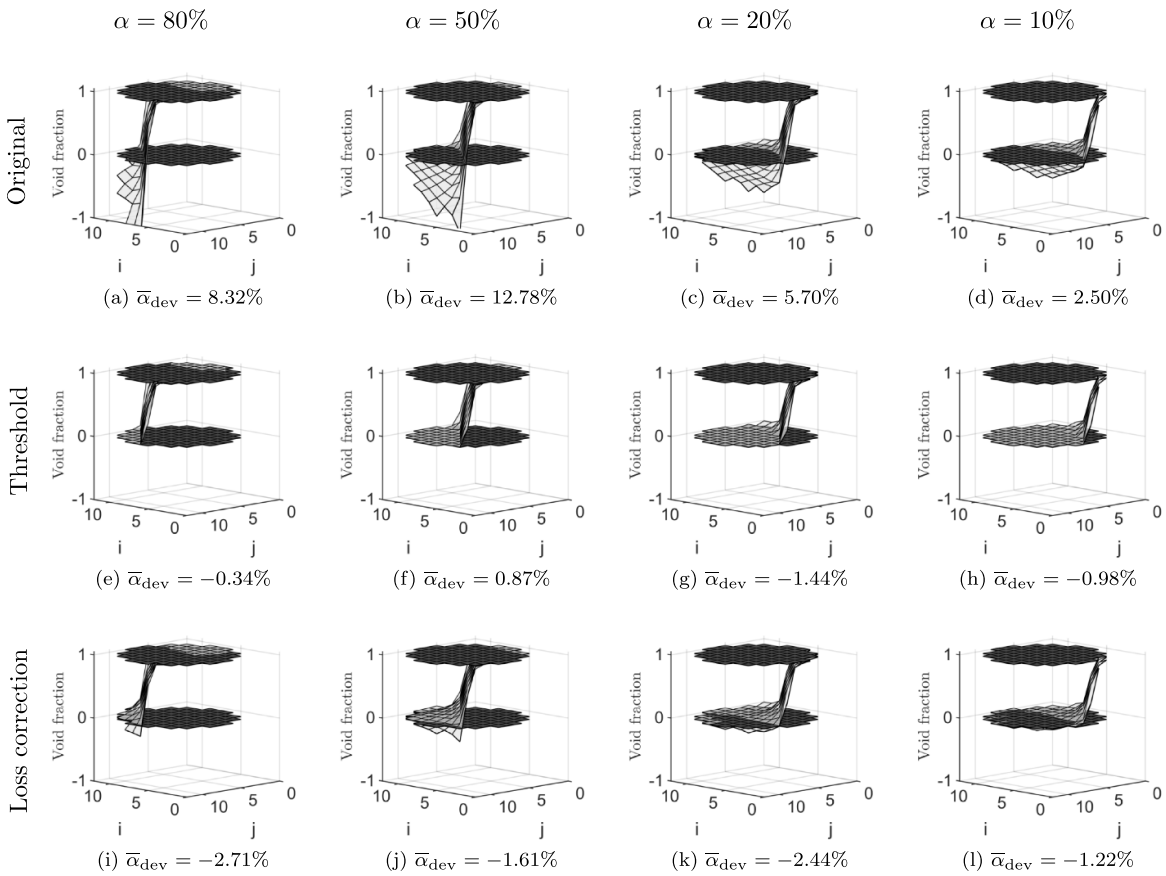

Figure 8. 3D view of the void fraction distribution (a)–(d) without correction; (e)–(h) using the cut-off procedure (equation (9)); and (i)–(l) using the proposed method of loss correction (equation (19)). The light gray surfaces represent the void fraction with the WMS containing water at different levels (conductivity of water $\sigma = 420\ \mu\text{S}\,\text{cm}^{-1}$).

4.2. Experimental validation

To evaluate the new method of loss correction, a real 12×12 WMS was filled with different levels of tap water ($\sigma = 420\ \mu\text{S}\,\text{cm}^{-1}$). Figure 8 shows 3D views of the phase fraction distribution obtained in the experiments. As expected, negative void fraction is observed in the experiments without correction (figures 8(a)–(d)). The critical cases are the experiments containing high void fraction, e.g. 80% and 50%. It happens because a low volume of conductive fluid inside the flow domain generates much less energy losses than the full calibration data. For this reason, the highest peaks of negative phase fraction are observed in such cases. On the other hand, the measurement containing 10% of void fraction presents voltage drop with similar magnitude and direction as the full reference data. Hence, losses from reference and operational measurement signals cancel each other out reducing the average phase fraction deviation. By correcting the void fraction through the threshold procedure (equation (9)) or using the proposed method (equations (18) and (19)), the phase fraction estimation is improved regardless of the water holdup.

By analyzing the average deviation of the cross-sectional void fraction $\overline{\alpha}_{\text{dev}}$ shown in figure 8, one could conclude that a threshold procedure is slightly better than the proposed method of loss correction. As can be seen, the local points containing negative phase fraction are cut-off, providing lower deviations compared to the new method. However, a threshold procedure works well only for some particular cases, e.g. when the phases are fully separated. If the phase distribution is complex such as in a dispersed flow, the information of small bubbles and droplets may be lost.

To illustrate this problem, WMS data of paraffin-water phantoms available in [25] were corrected using both threshold and loss correction methods. As can be seen in figure 9, the performance of the cut-off procedure is drastically reduced compared to the experiments where the fluids are fully separated, leading to average deviations of up to 10.37%. In contrast, by correcting the losses through a WMS with external references, the average deviation is decreased to less than 2% for all cases.

The performance of both methods can be better understood through figure 10, where local measurements along a vertical chord of the sensor are depicted (pattern 1). The reference data (dashed line) indicates that the local point $(10, 7)$ is filled by water-paraffin components. If the negative values of the original data are truncated by the cut-off method, this local point is inferred as 100% water, yielding a deviation of 19.89%. However, using the new method, the losses are compensated and the deviation is reduced to only 3.54% for the same point.

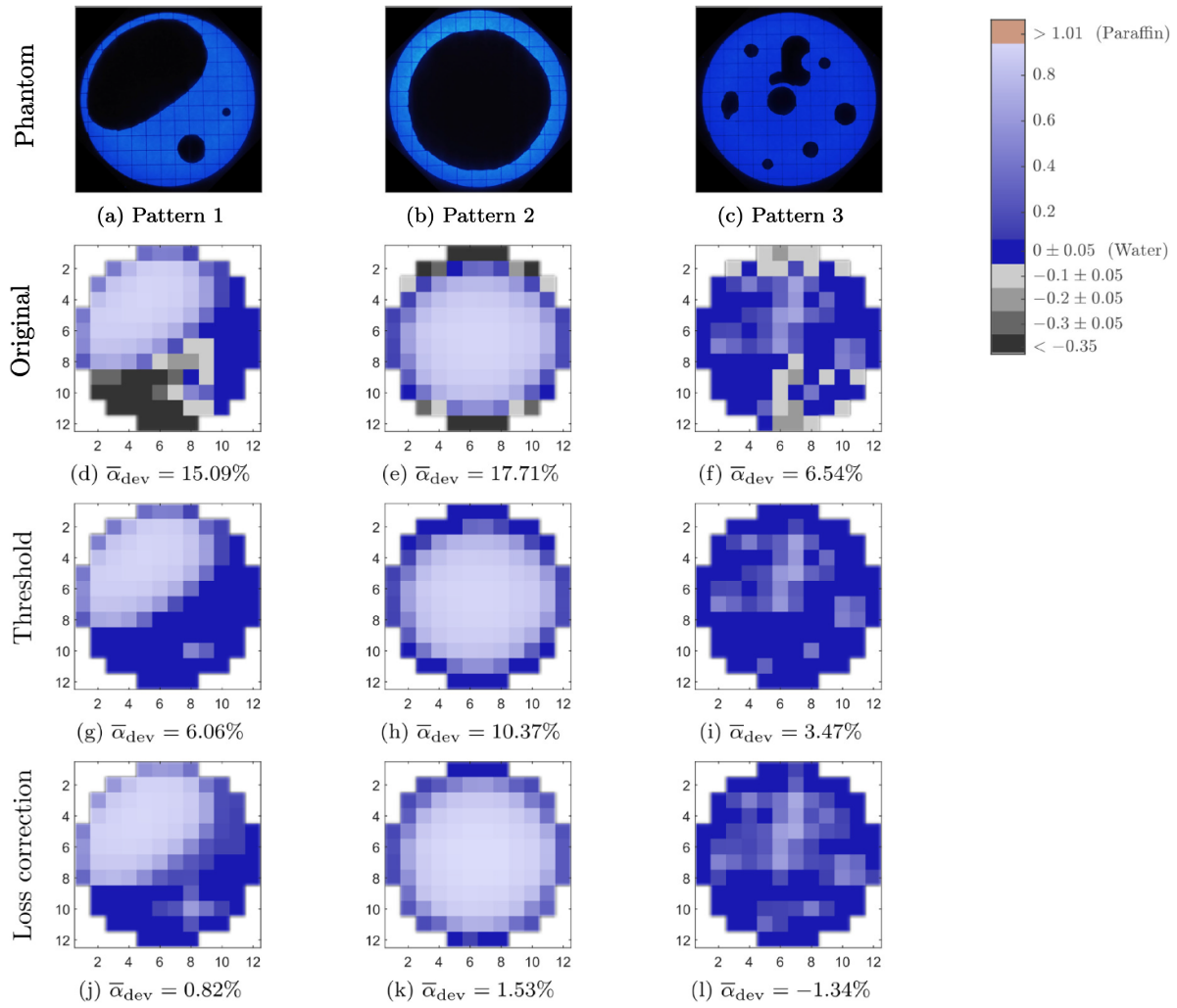

Figure 9. Phase fraction distribution of paraffin phantoms ($\varepsilon \approx 3.5$) submerged on water ($\varepsilon \approx 80$) obtained through a 12×12 WMS detectors for loss correction.

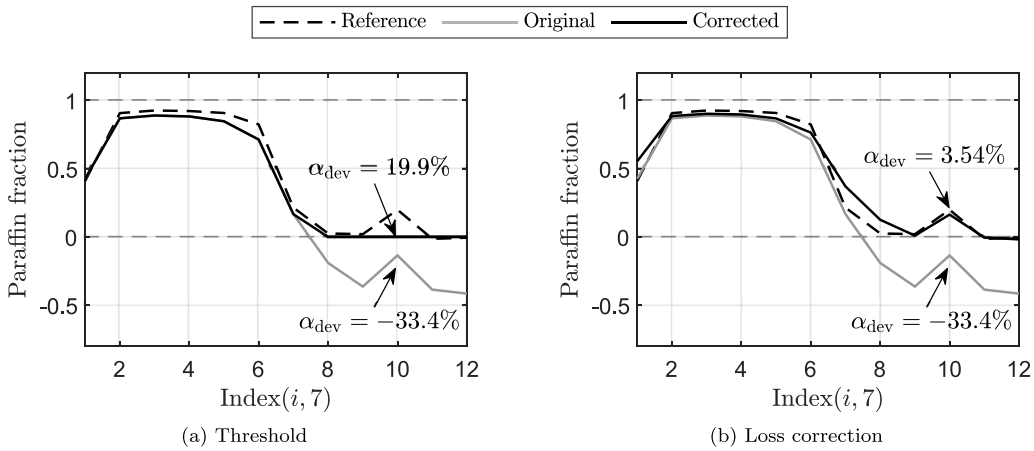

(a) Threshold (b) Loss correction

Figure 10. Local phase fraction along a vertical chord (column 7) of the phantom 1 (figure 9(a)). The void fraction is corrected by (a) threshold method and (b) the proposed procedure of loss correction.

As shown in figure 11, another advantage of the loss correction is the fact that local phase fraction deviations are greatly reduced if there are fluids with very different electrical conductivity in the sensor area, e.g. deionized and tap water. As mentioned in the previous section, this problem is hard to be solved only by circuit redesigns.

These experimental results show the high potential of the proposed method compared to the threshold and optimization

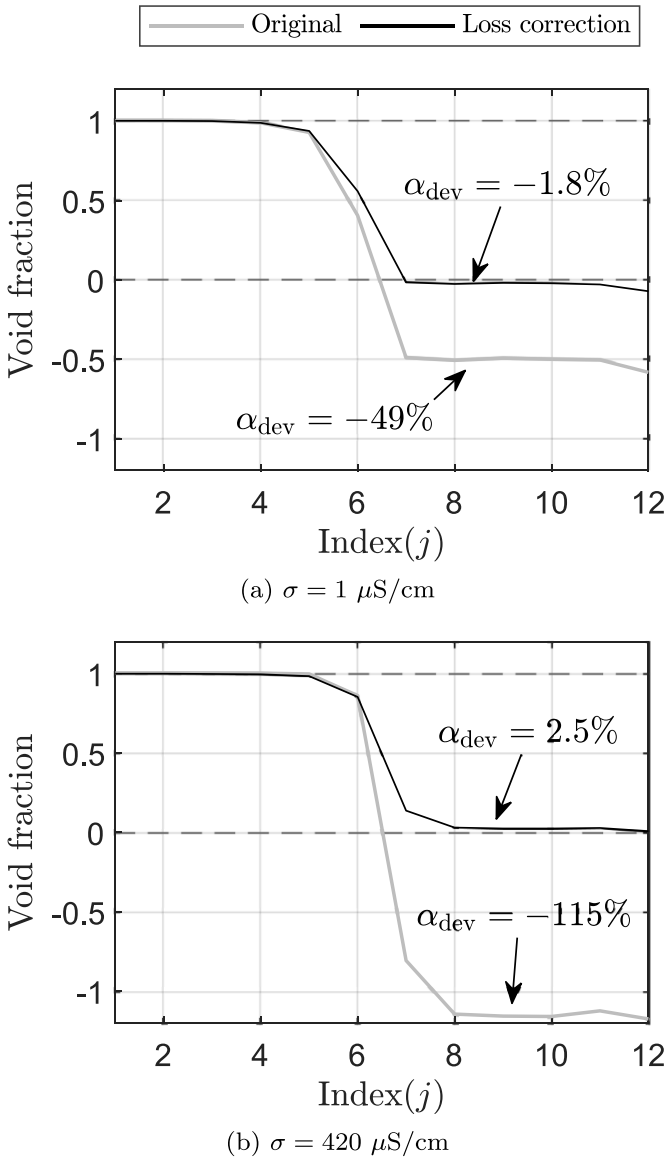

Figure 11. Local phase fraction along a vertical chord of a 12×12 WMS ($i = 6, j = 1$–12) containing 50% water. The void fraction is corrected independently of the electrical conductivity. (a) Deionized water; (b) tap water.

procedure. The reason for this is the capability of the proposed method to correct the phase fraction distribution of complex flow patterns even for fluids with very different electrical conducitvities. As explained earlier, the threshold method works well in flows where the phases are completely separated only, and overestimate measurement of mixtures containing small structures and interfaces. Hence, the method of loss correction is more recommended for measurement of flows with complex structures, e.g. oil-water emulsion/dispersion, foam, swarm of bubbles, etc.

5. Conclusion

In this paper, an analysis of the non-ideal characteristics of a WMS is presented. Based on an analytical model, the feedback gains of the sensor are optimized to reduce its measurement uncertainty. However, the optimization of the amplification circuit only does not hold if the dynamic range associated with the impedance of different fluids is extremely high (e.g gas and water), providing energy losses on WMS signals. Hence, an extended WMS with external reference impedances is proposed to estimate and correct WMS readings affected by losses. The main conclusions of this paper are summarized below:

WMSs measure electrical signals that are associated with the impedance of the fluid. In a typical gas-water flow, the dynamic range of the impedance for the different fluids is extremely high, so the amplifiers can become unbalanced if a fixed gain is used. When it happens, the potential on the negative input of the amplifiers differs from zero, so that the effects of crosstalk and losses due to the impedance of neighboring crossing-points are not fully suppressed. These effects in turn cause nonlinearities in the output signals being the major uncertainty source for WMS measurements. The following methods can be used to deal with this issue.

- High feedback gain + threshold: when selecting very high gains, the output signal gets closer to the upper limit of the amplifier providing a better SNR, which is critical for discriminating low impedance fluids such as gas and oil and also to discriminate small bubbles and droplets. However, by increasing the gains, the amplifiers depart from ideal and the phase fraction is underestimated reaching local and average deviations greater than 100% and 30%, respectively. If a threshold method is employed, negative phase fraction values are cut-off, improving the average cross-sectional phase fraction estimation. For specific flow regimes with large phase structures and interfaces, e.g. stratified flow, the average phase fraction becomes much smaller than the measurement uncertainty reported in the literature. For fluids with dispersed phases, it is possible to improve the average phase fraction by using alternative mixture models instead of the parallel, e.g. Maxwell, Maxwell-Garnett and logarithmic mixture models.
- Low gain without threshold: in this approach, the closed-loop gain is decreased, so that the amplifiers work at nearly optimal condition for fluids within a specific range of conductivity. In this paper, a gain optimization for tap water ($\sigma = 500$ μS cm^{-1}) was presented, achieving local phase fraction deviations lower than 6% and average phase fraction lower than 1% in stratified gas-water flow. However, if the same gains are used for deionized (1 μS cm^{-1}) and salty water (1000 μS cm^{-1}), the local and average void fractions are underestimated in the former and overestimated in the latter. Based on an analytical model, it was shown that the optimization of the gains only cannot fully suppress the effects of energy loss and crosstalk if the impedance of the neighboring crossing-points is too low, that is, if several crossing-points are submerged in conductive liquids or if the conductivity of the fluid is too high.
- Correction of energy loss: the new method proposed in this paper improves the accuracy of the sensor for a wide range of impedance. An additional transmitter wire is

embedded into the PCB layout outside the flow domain, so the external crossing-points are used to estimate and correct the energy losses in the output signals of the sensor. In the examples shown in this paper, local phase fraction deviations were reduced from -33.4% to less than 3.54% for fluid mixings with high dynamic range of their electrical conductivities—even for small phase structures. For complex two-phase flow patterns, the average phase fraction was reduced to 17.1%–1.53% in the worst case. Hence, the proposed method is more comprehensive than the others discussed above and has a high potential to provide accurate measurements of complex flows, such as oil-water emulsion/dispersion, foam, swarm of bubbles, etc which are commonly types of multiphase flows. Nevertheless, an amplifier with high GBW should be chosen and the feedback gain settings should be set to a good compromise before using the new approach. In addition, the use of a cut-off procedure can be also employed to improve the phase fraction estimation of large flow structures.

Although the experiments presented in this paper are focused only on the capacitance WMS [2], similar problems have also been observed for the conductivity wire-mesh senor [1], which will be subchecked in further works.

Data availability statement

The data that support the findings of this study are openly available at the following URL/DOI: https://doi.org/10.14278/rodare.897.

Acknowledgments

This research is funded by the European Social Fund and co-financed by tax funds based on the budget approved by the members of the Saxon State Parliament. Mr Dias is funded by the European Social Fund and the Free State of Saxony, Reference No. 100316833/100316834.

ORCID iDs

Felipe de Assis Dias https://orcid.org/0000-0002-8001-3404
Philipp Wiedemann https://orcid.org/0000-0003-0946-4656
Marco Jose da Silva https://orcid.org/0000-0003-1955-8293
Uwe Hampel https://orcid.org/0000-0002-7371-0148

References

[1] Prasser H-M, Böttger A and Zschau J 1998 A new electrode-mesh tomograph for gas–liquid flows *Flow Meas. Instrum.* **9** 111–9
[2] da Silva M J, Schleicher E and Hampel U 2007 Capacitance wire-mesh sensor for fast measurement of phase fraction distributions *Meas. Sci. Technol.* **18** 2245–51
[3] dos Santos E N, Schleicher E, Reinecke S, Hampel U and Da Silva M J 2015 Quantitative cross-sectional measurement of solid concentration distribution in slurries using a wire-mesh sensor *Meas. Sci. Technol.* **27** 15301
[4] Dias F D A, dos Santos E N, Da Silva M J, Schleicher E, Morales R E M, Hewakandamby B and Hampel U 2020 New algorithm to discriminate phase distribution of gas-oil-water pipe flow with dual-modality wire-mesh sensor—data set (available at: https://doi.org/10.14278/rodare.369)
[5] dos Santos E N, Vendruscolo T P, Morales R E M, Schleicher E, Hampel U and Da Silva M J 2015 Dual-modality wire-mesh sensor for the visualization of three-phase flows *Meas. Sci. Technol.* **26** 105302
[6] dos Santos E N, Da Silva M J, Morales R E M, Reinecke S, Schleicher E and Hampel U 2014 Dual-modality impedance wire-mesh sensor for investigation of multiphase flows *2014 IEEE Int. Conf. on Imaging Systems and Techniques (IST) Proc.* (IEEE) pp 316–9
[7] Hampel U, Otahal J, Boden S, Beyer M, Schleicher E, Zimmermann W and Jicha M 2009 Miniature conductivity wire-mesh sensor for gas-liquid two-phase flow measurement *Flow Meas. Instrum.* **20** 15–21
[8] Pietruske H and Prasser H-M 2007 Wire-mesh sensors for high-resolving two-phase flow studies at high pressures and temperatures *Flow Meas. Instrum.* **18** 87–94
[9] Prasser H-M and Häfeli R 2018 Signal response of wire-mesh sensors to an idealized bubbly flow *Nucl. Eng. Des.* **336** 3–14
[10] Tompkins C, Prasser H-M and Corradini M 2018 Wire-mesh sensors: a review of methods and uncertainty in multiphase flows relative to other measurement techniques *Nucl. Eng. Des.* **337** 205–20
[11] Wiedemann P, Dias F D A, Schleicher E and Hampel U 2020 Temperature compensation for conductivity-based phase fraction measurements with wire-mesh sensors in gas-liquid flows of dilute aqueous solutions *Sensors* **20** 7114
[12] Zhang H, Xiao Y and Gu H 2019 Numerical investigations of the accuracy of conductivity wire-mesh sensors *Nucl. Eng. Des.* **345** 148–56
[13] da Silva M J, dos Santos E N, Hampel U, Rodriguez I H and Rodriguez O M H 2011 Phase fraction distribution measurement of oil–water flow using a capacitance wire-mesh sensor *Meas. Sci. Technol.* **22** 104020
[14] Dias F D A, Pipa D R, Morales R E M and da Silva M J 2021 Wire-mesh sensor super-resolution based on statistical reconstruction *IEEE Trans. Instrum. Meas.* **70** 4503212
[15] Dias F D A, Wiedemann P, Da Silva M J, Schleicher E and Hampel U 2021 Combined finite element and electronic circuit model of a wire-mesh sensor *IEEE Access* **9** 66309–22
[16] Dias F, Wiedemann P, da Silva M, Schleicher E and Hampel U 2021 Tuning capacitance wire-mesh sensor gains for measurement of conductive fluids [optimierung eines kapazitiven gittersensors für die messung von leitfähigen flüssigkeiten] *Tech. Mess.* **88** S107–13
[17] Barsoukov E and Macdonald J 2005 *Impedance Spectroscopy: Theory, Experiment and Applications* (New York: Wiley)
[18] da Silva M J 2008 *Impedance Sensors for Fast Multiphase Flow Measurement and Imaging* (Dresden: TUD Press)
[19] Teletronic 2013 Wire-mesh sensor system: CAP200 manual (available at: https://hzdr-innovation.de/en/products/flow-measurement-technology/wire-mesh-sensor/)
[20] Thorn R, Johansen G A and Hjertaker B T 2012 Three-phase flow measurement in the petroleum industry *Meas. Sci. Technol.* **24** 12003

[21] Prasser H-M, Krepper E and Lucas D 2002 Evolution of the two-phase flow in a vertical tube—decomposition of gas fraction profiles according to bubble size classes using wire-mesh sensors *Int. J. Therm. Sci.* **41** 17–28
[22] Franco S 2002 *Design with Operational Amplifiers and Analog Integrated Circuits* vol 1988 (New York: McGraw-Hill)
[23] Filho J B S, Costa C A M, Cunha G C L, Belfort D R, Catunda S Y C, dos Santos E N and da Silva M J 2016 Requirements for an integrated conditioning circuit for multiphase flow imaging using impedance wire-mesh sensors *2016 IEEE 7th Latin American Symp. on Circuits Systems (LASCAS)* pp 291–4
[24] Gamio J C, Yang W Q and Stott A L 2001 Analysis of non-ideal characteristics of an ac-based capacitance transducer for tomography *Meas. Sci. Technol.* **12** 1076–82
[25] Dias F D A, Wiedemann P, Da Silva M J, Schleicher E and Hampel U 2021 Numerical and experimental data set obtained from paraffin phantom measurements based on the capacitance wire-mesh sensor (available at: https://doi.org/10.14278/rodare.898)